Published in final edited form as:

IEEE Trans Ultrason Ferroelectr Freq Control. 2014 July ; 61(7): 1171–1178. doi:10.1109/TUFFC.2014.3016.

Micromachined PIN-PMN-PT Crystal Composite Transducer for High-Frequency Intravascular Ultrasound (IVUS) Imaging

Xiang Li [Member, IEEE],
NIH Resource on Medical Ultrasonic Transducer Technology, Department of Biomedical Engineering, University of Southern California, Los Angeles, CA

Teng Ma,
NIH Resource on Medical Ultrasonic Transducer Technology, Department of Biomedical Engineering, University of Southern California, Los Angeles, CA

Jian Tian [Senior Member, IEEE],
H.C. Materials Corp., Bolingbrook, IL

Pengdi Han [Member, IEEE],
H.C. Materials Corp., Bolingbrook, IL

Qifa Zhou [Senior Member, IEEE], and
NIH Resource on Medical Ultrasonic Transducer Technology, Department of Biomedical Engineering, University of Southern California, Los Angeles, CA

K. Kirk Shung [Fellow, IEEE]
NIH Resource on Medical Ultrasonic Transducer Technology, Department of Biomedical Engineering, University of Southern California, Los Angeles, CA

Abstract

In this paper, we report the use of micromachined $PbIn_{1/2}Nb_{1/2}O_3$–$PbMg_{1/3}Nb_{2/3}O_3$–$PbTiO_3$ (PIN-PMN-PT) single crystal 1–3 composite material for intravascular ultrasound (IVUS) imaging application. The effective electromechanical coupling coefficient $k_{t(\text{eff})}$ of the composite was measured to be 0.75 to 0.78. Acoustic impedance was estimated to be 20 MRayl. Based on the composite, needle-type and flexible-type IVUS transducers were fabricated. The composite transducer achieved an 86% bandwidth at the center frequency of 41 MHz, which resulted in a 43 μm axial resolution. *Ex vivo* IVUS imaging was conducted to demonstrate the improvement of axial resolution. The composite transducer was capable of identifying the three layers of a cadaver coronary artery specimen with high resolution. The PIN-PMN-PT-based composite has superior piezoelectric properties comparable to PMN-PT-based composite and its thermal stability is higher than PMN-PT. PIN-PMN-PT crystal can be an alternative approach for fabricating high-frequency composite, instead of using PMN-PT.

qifazhou@usc.edu.

I. Introduction

HIGH-FREQUENCY ultrasonic transducers utilize very thin layers of piezoelectric material to generate and receive ultrasonic waves to image biological tissues with microscopic resolution. Its medical applications include dermatology, ophthalmology, cartilage imaging, blood flow measurement, and intravascular imaging [1]. Catheter-based intravascular ultrasound (IVUS) imaging is a widely used method for diagnosing coronary artery diseases, which are the number one killer in the United States [2]. An IVUS catheter normally incorporates a tiny high-frequency (20 to 80 MHz) single-element transducer with a rotational shaft to generate radial format cross-sectional images of coronary artery. IVUS provides detailed evaluation of lumen size, vessel remodeling, and plaque morphology [1], [3]. For IVUS, image resolution, penetration depth and dynamic range are crucial parameters that can strongly affect diagnosis accuracy.

Imaging resolution is inversely proportional to the frequency bandwidth of the transducers. Transducers with higher center frequency and broader bandwidth can provide better image resolution [1]. In our previous work, 80-MHz IVUS transducers were investigated and could provide axial resolution of 35 μm and penetration of 2 mm [4]. The fine resolution is critical for detecting certain vulnerable plaques such as thin-cap fibroatheroma (TCFA), which has a cap thickness less than 65 μm [5]. The drawback of working at 80 MHz is the shallow penetration depth resulting from the strong attenuation in blood and vessel wall. An alternative method to improve resolution without sacrificing penetration depth is to use transducers with broader bandwidth at relatively lower frequency (40 MHz). Moreover, a broadband transducer is advantageous for multi-frequency signal processing to differentiate blood and vessel [6].

To achieve optimal imaging performance, the piezoelectric material of an IVUS transducer must be carefully chosen. Conventionally, $Pb(Zr,Ti)O_3$ (PZT)-based ceramics, such as PZT-5H, have been used for fabricating IVUS transducers. Recently, binary relaxor-based ferroelectric single-crystal $Pb(Mg_{1/3}Nb_{2/3})$–$PbTiO_3$ (PMN-PT) has also been investigated for fabricating high-frequency ultrasonic transducers [7], [8]. Compared with PZT ceramics, PMN-PT crystal demonstrated improved sensitivity and bandwidth, resulting from its higher piezoelectric coefficient (d_{33} ~2000 pm/V), and electromechanical coupling coefficients (k_t ~ 0.58, k_{33} ~ 0.9) [9]–[12]. Ceramic or crystal 1–3 composite material exhibits even broader bandwidth than monolithic materials because of composite's very high coupling coefficient and low acoustic impedance [13]. However, composites for transducers operating above 20 MHz cannot be made using traditional dice-and-fill technique because of the thickness limitation of the dicing saw blade, which is no less than 10 μm [14]–[16]. Mechanical dicing can also produce highly stressed and damaged surface layers, thereby degrading the properties of 1–3 composites [17].

For 1–3 composites, the frequency of the first lateral mode is empirically expressed as

$$f_{\mathrm{l}}=\frac{V_{\mathrm{T}}}{2\sqrt{2}d_{\mathrm{p}}}, \quad (1)$$

where f_l is the frequency of first lateral mode resonance, V_T is the shear wave velocity of filler, and d_P is the kerf width [18], [19]. Generally, the kerf width is chosen to ensure that the lateral resonance is at least twice the center frequency. For composites working at 40 MHz or higher, the kerf must be less than 6 μm to achieve a bandwidth larger than 70%. More recently, micromachining techniques such as deep reactive ion etching (DRIE) have been adopted to fabricate fine-kerf composites and build high-frequency ultrasonic transducers. Liu *et al*. and Sun *et al*. reported micromachined PMN-PT 1–3 composite for fabricating single-element and annular array transducers for ultrasonic imaging [20], [21]. Yuan *et al*. and Jiang *et al*. reported PMN-PT 1–3 composites with 4 μm kerf and effective k_t values of 0.67 to 0.83 for IVUS application [7], [18], [19], [21]–[23]. The acoustic impedance of the composite was as low as 20 MRayl. Based on the composite material, piezocomposite microfabricated ultrasound transducers (PC-MUT) were built at 15 to 75 MHz with broad bandwidth (77% to 90%) and high sensitivity. Compared with monolithic ceramic or crystal transducers, bandwidth was greatly improved.

However, previously reported micromachined 1–3 composites were fabricated from PMN-PT crystal. The binary PMN-PT crystal has relatively low coercive field (E_c ~ 2.5 kV/cm), depoling temperature ($T_{R/T}$ ~ 60°C to 95°C), and Curie temperature (T_c ~ 130°C to 178°C) [24]–[27]. Higher E_c would allow transducers to be driven in a higher electrical field and higher $T_{R/T}$ for a broader temperature usage range [26], [27]. During the fabrication process, transducers are frequently incubated at elevated temperatures (40°C to 90°C) for epoxy curing, wax bonding, electrode sputtering, etc., which can cause PMN-PT depoling. Depoling can make testing transducer during fabrication inconvenient. In addition, an IVUS catheter must go through a sterilization process before entering the market. Some sterilization processes, such as steam sterilization, work at relatively high temperature (90°C). After sterilization, it is difficult to repole the IVUS transducer without taking the catheter out of the sterilized pouch. Therefore, thermal instability of PMN-PT may degrade transducers' performance during fabrication and sterilization processes. By adding lead indium niobate (PIN) into the PMN-PT system, the ternary crystal PIN-PMN-PT was found to have superior electrical and thermal stability (E_c ~ 5.5 to 6 kV/cm, $T_{R/T}$ ~120°C to 130°C, T_c ~160°C to 200°C) to overcome the aforementioned drawbacks, while maintaining the excellent piezoelectric properties (d_{33} ~ 900 to 1900 pm/V, k_{33} ~ 0.83 to 0.92) [26], [27]. PIN-PMN-PT has been investigated for high-frequency ultrasonic applications and demonstrated reduced temperature dependence of performance and minimal depolarization during fabrication [28], [29]. Composites based on PIN-PMN-PT crystal inherit the improvements of the thermal and electrical properties [19].

Considering the merits of higher usage temperature range and coercive field, PIN-PMN-PT could be more advantageous than PMN-PT to fabricate micromachined 1–3 composite for high frequency IVUS applications. In this paper, we report the use of micromachined PIN-PMN-PT 1–3 composite material for IVUS application. Miniature side-looking needle transducers and flexible IVUS catheters were built from the composite to operate at 40 MHz. *Ex vivo* experiments were conducted to demonstrate the superiority of the composite for IVUS application.

II. Acoustic Stacks Characterization

PIN-PMN-PT crystal 1–3 composite was fabricated using inductively coupled plasma (ICP)-enhanced DRIE technique by H. C. Materials Corp. [19]. Polished PIN-PMN-PT crystal plate was first coated with Cr/Au as the seed layer for subsequent nickel electroplating. Photolithography was used to lay out the etching pattern over the Cr/Au layer. A 4- to 5-μm-thick nickel mask was then electroplated with the inverse pattern of the photoresist. Crystal parts with the patterned nickel mask were loaded in ICP-enhanced plasma (Oxford Instruments, PlasmaLab 100, Abingdon, Oxford, UK) for DRIE. Following etching, kerfs in the etched crystals were filled with epoxy (EPO-TEK 301, Epoxy Technology Inc. Billerica, MA). After epoxy cures, the composite was lapped from both sides to the final thickness. The composite plate was sputtered with Cr/Au electrodes on both sides and then deposited with a thick conductive backing material. A cross-sectional micrograph of the composite on top of a thick conductive backing material is shown in Fig. 1. The thickness of the composite is around 27 μm and the kerf width is less than 5 μm. DRIE produces a near vertical etched profile with a side wall angle greater than 85°.

The composite (with backing) was diced into 0.5 × 0.4 mm stacks to build IVUS transducers. The stacks were poled with a dc electric field of 20 kV/cm for 5 min at room temperature. Dielectric properties of the stacks were measured with an impedance analyzer (Agilent Technologies Inc., Santa Clara, CA). The frequency dependence of the electrical impedance and phase were measured from 10 MHz to 110 MHz, as shown in Fig. 2. The effective electromechanical coupling coefficient $k_{t(\text{eff})}$ was calculated according to the *IEEE Standard on Piezoelectricity*:

$$k_t = \sqrt{\frac{\pi}{2} \cdot \frac{f_s}{f_p} \tan\left(\frac{\pi}{2} \cdot \frac{f_p - f_s}{f_p}\right)}, \quad (2)$$

where f_s and f_p are series and parallel resonant frequencies [30]. f_s and f_p were 44 MHz and 63 MHz in Fig. 2. $k_{t(\text{eff})}$ was 0.75 to 0.78 for ten measured composite stacks. The values were comparable to those achieved in PMN-PT composite (0.67 to 0.83) [7], [18], [19], [21]–[23]. The acoustic impedance (Z) can be calculated according to

$$Z = \rho \cdot c = \rho \cdot 2t \cdot f_p, \quad (3)$$

where ρ is the density of composite, which can be estimated by the volume fraction (70% to 80%) of crystal, c is the speed of sound in the composite, t is the thickness of the composite. The acoustic impedance of the composite material was estimated to be between 20 and 22 MRayl, which was close to the value of PMN-PT composite reported by Sun *et al.* (18 MRayl) and Yuan *et al*. (20 MRayl) [21], [22].

To evaluate the thermal stability of the piezoelectric property, composite stacks were incubated for 10 min at several temperatures in the range of 20°C to 150°C at increments of 20°C. Electrical impedance and phase were measured at each temperature, as shown in Fig. 3. The results showed that electrical impedance slightly changed below 100°C, then the impedance peaks started to decrease, but still maintained significant piezoelectricity until

130°C. The results were consistent with the $T_{R/T}$ (~120°C to 130°C) of PIN-PMN-PT. The impedance peaks vanished above 140°C, which is close to the T_c (160°C to 200°C) of PIN-PMN-PT. The change of $k_{t(\text{eff})}$ value was shown in Fig. 4 as the solid line. Note that although k_t may not change dramatically when below $T_{R/T}$, the electrical impedance peak actually started to decrease before temperature reached $T_{R/T}$. For comparison, one PMN-PT single crystal stack (with matching/backing at the size of 0.5 × 0.4 mm) was also treated in the same manner; its k_t is plotted as the dashed line in Fig. 4. For PIN-PMN-PT composite, the $k_{t(\text{eff})}$ value did not show significant change until temperature increased to 140°C. For PMN-PT crystal, the k_t value was lower, and dropped quickly when above 80°C. Both PIN-PMN-PT and PMN-PT can be repoled in dc electrical fields at room temperature.

The epoxy filler has a glass point of 65°C, above which the epoxy becomes more deformable. However, if no external pressure applied, the composite can maintain its structure. After testing the composite material at 140°C, the composite can be re-poled to recover piezoelectricity at room temperature. During the transducer fabrication process, the composite is normally treated under 100°C. In such conditions, we did not observe composite deformation caused by thermal expansion.

III. IVUS Transducer Fabrication and Characterization

Side-viewing needle-type IVUS transducers and flexible catheter-type IVUS transducers were fabricated based on the PIN-PMN-PT 1–3 composite. For the needle transducer, a diced composite stack was housed within a polyimide tube, on the side of which a window was opened to allow the transducer to be mounted. A 0.25-mm outer diameter (OD) 50-Ω coaxial wire (Tyco Electronic, Berwyn, PA) was connected to the composite backing using conductive epoxy inside the polyimide tube, which provided electrical insulation from the outer stainless steel needle housing. A window was opened on the side of the needle housing (OD: 0.92 mm) for acoustic waves to go through. Fast-cure epoxy was filled into the gap between the composite stack and needle housing to insulate the inner electrode. Cr/Au electrode was sputtered over the composite surface and stainless steel housing to form the ground connection. A Parylene (Specialty Coating Systems, Indianapolis, IN) layer (10 ± 0.5 μm) was vapor-deposited onto the transducer to serve as a matching and waterproofing layer. The transducer was finally connected to a brass holder and SMA connector for electrical connection. The needle IVUS transducer is shown in Fig. 5(a). Another flexible version was fabricated with a double-wound flexible torque coil (OD: 0.65 mm, Asahi Intecc USA Inc., Santa Ana, CA), as shown in Fig. 5(b). The torque coil allows for smooth torque translation to the distal end through the entire catheter.

The transducer's performance was measured in a deionized water bath at room temperature. The pulse–echo test was conducted with an X-cut quartz as a signal reflecting target at a standoff distance of 2 mm, in the transducer's far-field range to avoid near-field diffraction. A broadband negative pulse with approximately 100 V_{pp} emitted from a pulser/receiver unit (Panametrics PR5900, Olympus NDT, Inc., Waltham, MA) was used to excite the transducer. Echo signals were received by the same unit, and then digitized by a 1-GHz oscilloscope (LC534, LeCroy Corp., Chestnut Ridge, NY). The frequency response of the

transducer was analyzed from the echo waveform, shown in Fig. 6. Center frequency (f_c) and −6-dB fractional bandwidth (BW) were determined by

$$f_c = \frac{f_l + f_u}{2} \quad (4)$$

$$\mathrm{BW} = \frac{f_u - f_l}{f_c} \times 100\%, \quad (5)$$

where f_l and f_u are defined as lower and upper −6-dB frequencies, at which the magnitude of the spectrum is 50% (−6-dB) of the maximum. As shown in Fig. 6, the echo signal had short pulse duration and small ring down. The measured f_c was 41 MHz and BW was 86%. BW is comparable to the reported PMN-PT composite transducer (77% to 90%) [7], [21]–[23], but almost doubled that of a PMN-PT crystal transducer (45%) [31].

Two-way insertion loss (IL) was calculated using the ratio of transmitting and receiving voltage amplitudes, then compensated for the attenuation in water (2.2×10^{-4} dB/mm × MHz^2) and loss caused by the imperfect reflection from the quartz target (1.9 dB) [32]. Because the quartz target is in the far-field range, no compensation for diffraction loss was included. Insertion loss values were measured using 20-cycle sinusoid bursts and sweeping frequency from 15 MHz to 75 MHz, at 5 MHz increments. The insertion loss was calculated using

$$\mathrm{IL} = 20log\frac{V_R}{V_T} + 1.9 + 2.2 \cdot 10^{-4} \cdot 2d \cdot f_c^2, \quad (6)$$

where f_c is center frequency (in megahertz), V_T and V_R are transmitting and receiving amplitudes (in volts), and d is the distance (in millimeters) between target and transducer. The two-way IL is shown in Fig. 7. At 40 MHz, the value is measured to be 17 dB, which is comparable to the IL of both PMN-PT composite transducer (18 dB) and single-crystal transducer (15 dB) of similar size [21], [31].

Tungsten wire targets with 6 μm OD were imaged to determine axial and lateral resolutions of the transducer, as shown in Fig. 8(a). The image has 1000 scan lines with a step size of 10 μm. For comparison, the wire targets were also imaged by a 40-MHz PMN-PT single-crystal transducer (two matching layers; one backing layer; 0.5 × 0.4 mm aperture; unfocused; 47% BW [31]), as shown in Fig. 8(b). The axial and lateral resolutions were determined from the −6-dB envelope width from the wire located at 1.3 mm, which is close to the transducer's natural focus (1.1 mm). For the PIN-PMN-PT composite transducer, axial and lateral resolutions were 43 μm and 226 μm, respectively. For the PMN-PT single-crystal transducer, axial and lateral resolutions were 62 μm and 278 μm. As shown in Fig. 8, the wire phantom images of the composite transducer were much thinner than those of the single-crystal transducer because of the improved axial resolution. Images are displayed with 50 dB dynamic range.

IV. IVUS System Setup and Imaging Experiments

To test the PIN-PMN-PT composite transducer for intravascular imaging, *ex vivo* imaging of postmortem human coronary artery specimens was performed. The imaging system is illustrated in Fig. 9. A pulser/receiver (Panametrics PR5900, Olympus NDT Inc., Waltham, MA) is used to excite the transducer and receive echo signals. RF data are digitized by a 12-bit data acquisition board (Gage Applied Technologies, Lockport, IL) with a sampling rate of 400 MHz. An IVUS transducer is mounted to a custom-built rotational joint, which translates torque from the motor to the transducer and couples the electrical signal to the pulser/receiver. The rotational motor provides trigger signals at every step to trigger a function generator, which then synchronizes the pulser/receiver and data acquisition board. The scanning procedure is controlled by a LabVIEW (National Instruments, Austin, TX) program. RF data are saved and post-processed for image display by Matlab (The MathWorks Inc., Natick, MA). Images are displayed with 50 dB dynamic range.

During the imaging experiment, the tip of a transducer was positioned inside the artery specimen, which stood in a water tank. Scanning was achieved by rotating the transducer while the specimen was kept immobile. An *ex vivo* IVUS image from the composite transducer is shown in Fig. 10(a). For comparison, an image of the artery from the PMN-PT crystal transducer of the same cross section is shown in Fig. 10(b). Both images are capable of differentiating the thickened intima (I), media (M), and adventitia (A) layers, as well as visualizing the calcified plaques (Ca, high intensity areas followed by acoustic shadow). However, because of the improved axial resolution of composite transducer, Fig. 10(a) displays higher clarity (finer speckles) of all the three layers. The boundaries of IM and MA (denoted by green arrows) were identifiable by the composite transducer in Fig. 10(a), but are blurred in Fig. 10(b) and even unidentifiable at 9 to 11 o'clock. The improved resolution is also helpful to accurately determine the percentage of calcified plaque over the entire lumen circumference.

V. Conclusion

In this paper, we reported the use of micromachined PIN-PMN-PT single-crystal 1–3 composite for IVUS imaging application. The composite material demonstrated improved effective electromechanical coupling coefficient $k_{t(\text{eff})}$ compared with monolithic single crystal. The usage temperature of the composite is at least 30°C higher than PMN-PT. The acoustic impedance is as low as 20 MRayl. Using the composite, needle-type and flexible-type IVUS transducers were fabricated and tested. 41-MHz transducers with 86% bandwidth were achieved, which resulted in 43 μm axial resolution. The characterization results of PIN-PMN-PT crystal composite showed superior piezoelectric properties which were comparable to that of PMN-PT based crystal composite, as well as improved thermal property compared with that of PMN-PT based composite. PIN-PMN-PT crystal can be an alternative approach for fabricating high-frequency composite. *Ex vivo* IVUS imaging was conducted to demonstrate the superiority of improved axial resolution. The composite transducer was able to identify the three layers of a human coronary artery specimen with high definition, whereas the image from a single-crystal transducer showed lower clarity of the layered structures.

In conclusion, we have demonstrated the feasibility of using PIN-PMN-PT composite for IVUS imaging. The composite holds great potential for improving current IVUS imaging technology.

Acknowledgments

The authors wish to thank Dr. J.-S. Jeong for transducer fabrication and Ms. J. Yin for providing the tissue samples. The authors thank individuals who donated their bodies and tissues for the advancement of education and research.

This work was supported by National Institute of Health (NIH) grant number P41-EB002182.

Biographies

Xiang Li received a B.E. degree from Zhejiang University, Hangzhou, China, in 2007, and M.S. and Ph.D. degrees from the University of Southern California (USC), Los Angeles, CA, in 2010 and 2012, respectively. He started his Ph.D. study in 2008 with the support of the USC Provost's Fellowship under the direction of Dr. K. Kirk Shung and Dr. Qifa Zhou in the NIH Ultrasonic Transducer Resource Center (UTRC). In 2010, he won the Student Paper Competition Award at the IEEE International Ultrasonics Symposium, San Diego, CA. His research interest includes medical ultrasound technology, intravascular ultrasound (IVUS) imaging, integrated IVUS-OCT imaging, and intravascular photoacoustic imaging. He has published 25 peer-reviewed journal papers and 20 conference papers.

Teng Ma received his B.S.E degree in biomedical engineering from the University of Michigan, Ann Arbor, MI, in 2011. He received his M.S. degree in biomedical engineering from the University of Southern California, Los Angeles, CA, in 2013. He joined the NIH Resource Center for Medical Ultrasonic Transducer Technology as a Research Assistant and Ph.D. candidate under the supervision of Dr. K. Kirk Shung and Dr. Qifa Zhou. In 2013, two of his papers were selected as Best Student Paper Finalists and were featured in the 2013 Joint UFFC, EFTF, and PFM Symposium. His research interests include medical ultrasound technology and multi-modality intravascular imaging by combining ultrasonic and optical

techniques, such as intravascular ultrasound (IVUS), intravascular optical coherence tomography (IV-OCT), intravascular photoacoustic imaging (IVPA), and acoustic radiation force optical elastography (ARF-OCE). He is also actively working in translational research and medical device commercialization with an entrepreneurial spirit to translate innovative technology from research to clinical benefits.

Jian Tian (M'06–SM'11) received a B.Sc.(Hons) degree in geology and an M.S. degree in geochemistry from Peking University, Beijing, China. He received a Ph.D. degree in geology and an M.S. degree in materials science and engineering from the University of Illinois at Urbana-Champaign, Urbana, IL. He is the Director of Single Crystal Technology at H. C. Materials Corporation, Bolingbrook IL. His research interests include crystal growth of PMNPT- based piezoelectric single crystals, new composition development, crystal physics, high-frequency crystal composites, and applications of piezoelectric crystals and crystal composite materials.

Pengdi Han (M'90) is one of the pioneers of large-scale multi-crucible Bridgman method crystal growth, and is the founder of H. C. Materials Corporation in Bolingbrook, IL. After being awarded his B.Sc. degree in electrical engineering from Wuhan University of Technology in 1964, he joined the crystal growth group of synthetic fluorine mica in the Shanghai Ceramic Institute, China. He became a Research Associate in the Research Institute of Synthetic Crystals in Beijing, China, after completing his graduate studies in the theory of crystal growth in the Chemistry Department of Shandong University, China, in 1978. He was awarded three Outstanding Research Prizes from the State Science Committee of China. He served as the Director of the Department of Functional Crystals and a Member of the Scientific Committee in the Research Institute of Synthetic Crystals from 1979 to 1986. He joined Professor David Payne's group as a Senior Research Scientist at the University of Illinois at Urbana-Champaign, from 1987 to 2000. His research interests include crystal growth and crystal physics. He has authored more than 120 papers, one book, and three patents.

Qifa Zhou received his Ph. D. degree from the Department of Electronic Materials and Engineering of Xi'an Jiaotong University, China in 1993. He is currently a Research Professor at the NIH Resource on Medical Ultrasonic Transducer Technology and the Department of Biomedical Engineering and Industry & System Engineering at the University of Southern California (USC), Los Angeles, CA. Before joining USC in 2002, he worked in the Department of Physics at Zhongshan University in China, the Department of Applied Physics, Hong Kong Polytechnic University, and the Materials Research Laboratory, Pennsylvania State University. Dr. Zhou is a senior member of the IEEE Ultrasonics, Ferroelectrics, and Frequency Control (UFFC) Society and a member of the UFFC Society's Ferroelectric Committee. He is also a member of the Technical Program Committee of the IEEE International Ultrasonics Symposium. He is an Associate Editor of the *IEEE Transactions on Ultrasonics, Ferroelectrics, and Frequency Control*. His current research interests include the development of ferroelectric thin films, MEMS technology, nano-composites, and modeling and fabrication of high-frequency ultrasound transducers and arrays for medical imaging applications, such as photoacoustic imaging and intravascular imaging. He has published more than 130 journal papers in this area.

K. Kirk Shung obtained a B.S. degree in electrical engineering from Cheng-Kung University in Taiwan in 1968; an M.S. degree in electrical engineering from the University of Missouri, Columbia, MO, in 1970; and a Ph.D. degree in electrical engineering from the University of Washington, Seattle, WA, in 1975. He taught at The Pennsylvania State University, University Park, PA, for 23 years before moving to the Department of Biomedical Engineering, University of Southern California, Los Angeles, CA, as a professor in 2002. He has been the director of the NIH Resource on Medical Ultrasonic Transducer Technology since 1997. Dr. Shung is a life fellow of IEEE and a fellow of the Acoustical Society of America and the American Institute of Ultrasound in Medicine. He is a founding fellow of the American Institute of Medical and Biological Engineering. He received the IEEE Engineering in Medicine and Biology Society Early Career Award in 1985 and was the coauthor of a paper that received the best paper award for the *IEEE Transactions on*

Ultrasonics, Ferroelectrics, and Frequency Control (UFFC) in 2000. He was elected an outstanding alumnus of Cheng-Kung University in Taiwan in 2001. He was selected as the distinguished lecturer for the IEEE UFFC society for 2002–2003. He received the Holmes Pioneer Award in Basic Science from the American Institute of Ultrasound in Medicine in 2010. He was selected to receive the academic career achievement award from the IEEE Engineering in Medicine and Biology Society in 2011.

Dr. Shung has published more than 400 papers and book chapters. He is the author of the textbook *Principles of Medical Imaging*, published by Academic Press in 1992 and the textbook *Diagnostic Ultrasound: Imaging and Blood Flow Measurements*, published by CRC Press in 2005. He co-edited the book *Ultrasonic Scattering by Biological Tissues*, published by CRC Press in 1993. He is an associate editor of the *IEEE Transactions on Ultrasonics, Ferroelectrics, and Frequency Control* and a member of the editorial board of *Ultrasound in Medicine and Biology*. Dr. Shung's research interests are in ultrasonic transducers, high-frequency ultrasonic imaging, ultrasound microbeams, and ultrasonic scattering in tissues.

References

1. Foster FS, Pavlin CJ, Harasiewicz KA, Christopher DA, Turnbull DH. Advances in ultrasound biomicroscopy. Ultrasound Med Biol. 2000; 26(1):1–27. [PubMed: 10687788]
2. National Heart Lung and Blood Institute. What is atherosclerosis? [Online]. May 19. 2013 Available: http://www.nhlbi.nih.gov/health/health-topics/topics/atherosclerosis/
3. Pasterkamp G, Falk E, Woutman H, Borst C. Techniques characterizing the coronary atherosclerotic plaque: Influence on clinical decision making. J Am Coll Cardiol. 2000; 36(1):13–21. [PubMed: 10898406]
4. Li X, Wu W, Chung Y, Shih WY, Shih WH, Zhou QF, Shung KK. 80-MHz intravascular ultrasound transducer using PMN-PT free-standing film. IEEE Trans Ultrason Ferroelectr Freq Control. 2011; 58(11):2281–2288. [PubMed: 22083761]
5. Kolodgie FD, Burke AP, Farb A, Gold HK, Yuan JY, Narula J, Finn AV, Virmani R. The thin-cap fibroatheroma: A type of vulnerable plaque The major precursor lesion to acute coronary syndromes. Curr Opin Cardiol. 2001; 16(5):285–292. [PubMed: 11584167]
6. Li WG, Carrillo R, Yuan J, Teo TJ, Thomas L. Multifrequency processing for lumen enhancement with wideband intravascular ultrasound. IEEE Ultrasonics Symp. 2008:371–374.
7. Yuan J, Jiang X, Cao PJ, Sadaka A, Bautista R, Snook K, Rehrig PW. High frequency piezo-composites microfabricated ultrasound transducers for intravascular imaging. IEEE Ultrasonics Symp. 2006:264–268.
8. Rhee S. High-frequency (IVUS) ultrasound transducer technology—Applications and challenges. IEEE Int Symp Applications of Ferroelectrics. 2007:856–857.
9. Park SE, Shrout TR. Ultrahigh strain and piezoelectric behavior in relaxor based ferroelectric single crystals. J Appl Phys. 1997; 82(4):1804–1811.
10. Zhang SJ, Shrout TR. Relaxor-PT single crystals: Observations and developments. IEEE Trans Ultrason Ferroelectr Freq Control. 2010; 57(10):2138–2146. [PubMed: 20889397]
11. Tian J, Han PD, Payne DA. Measurements along the growth direction of PMN-PT crystals: Dielectric, piezoelectric, and elastic properties. IEEE Trans Ultrason Ferroelectr Freq Control. 2007; 54(9):1895–1902. [PubMed: 17941396]
12. Luo HS, Xu GS, Xu HQ, Wang PC, Yin ZW. Compositional homogeneity and electrical properties of lead magnesium niobate titanate single crystals grown by a modified Bridgman technique. Jpn J Appl Phys. 2000; 39(9B):5581–5585.
13. Smith WA. The role of piezocomposites in ultrasonic transducers. IEEE Ultrasonics Symp. 1989; 2:755–766.

14. Cheng KC, Chan HLW, Choy CL, Yin QR, Luo HS, Yin ZW. Single crystal PMN-0.33PT/epoxy 1–3 composites for ultrasonic transducer applications. IEEE Trans Ultrason Ferroelectr Freq Control. 2003; 50(9):1177–1183. [PubMed: 14561033]
15. Zhang YY, Zhao XY, Wang W, Ren B, Liu D, Luo HS. Fabrication of PIMNT/epoxy 1–3 composites and ultrasonic transducer for nondestructive evaluation. IEEE Trans Ultrason Ferroelectr Freq Control. 2011; 58(9):1774–1781. [PubMed: 21937308]
16. Zhou D, Cheung KF, Chen Y, Lau ST, Zhou QF, Shung KK, Luo HS, Dai JY, Chan HLW. Fabrication and performance of endoscopic ultrasound radial arrays based on PMN-PT single crystal/epoxy 1–3 composite. IEEE Trans Ultrason Ferroelectr Freq Control. 2011; 58(2):477–484. [PubMed: 21342833]
17. Lee HJ, Zhang SJ, Shrout TR. Scaling effects of relaxor-$PbTiO_3$ crystals and composites for high frequency ultrasound. J Appl Phys. 2010; 107(12) art. no. 124107.
18. Jiang X, Yuan J, Cheng A, Snook K, Cao PJ, Rehrig PW, Hackenberger WS, Lavalelle G, Geng X, Shrout TR. Microfabrication of piezoelectric composite ultrasound transducers (PC-MUT). IEEE Ultrasonics Symp. 2006:922–925.
19. Tian J, Meneou K, Stone B, Han P. Piezoelectric crystal composite for high frequency ultrasound application. IEEE Ultrasonics Symp. 2010:65–67.
20. Liu CG, Djuth F, Li X, Chen RM, Zhou QF, Shung KK. Micromachined high frequency PMN-PT/epoxy 1–3 composite ultrasonic annular array. Ultrasonics. 2012; 52(4):497–502. [PubMed: 22119324]
21. Sun P, Wu D, Zhu B, Hu C, Liu C, Djuth FT, Zhou Q, Wang G, Shung KK. High frequency PMN-PT 1–3 composite transducer for ultrasonic imaging application. Ferroelectrics. 2010; 408(1):120–128. [PubMed: 21869845]
22. Yuan J, Rhee S, Jiang XN. 60 MHz PMN-PT based 1–3 composite transducer for IVUS imaging. IEEE Ultrasonics Symp. 2008:682–685.
23. Jiang X, Snook K, Cheng A, Hackenberger WS, Geng X. Micromachined PMN-PT single crystal composite transducers—15–75 MHz PC-MUT. IEEE Ultrasonics Symp. 2008:164–167.
24. Park SE, Shrout TR. Characteristics of relaxor-based piezoelectric single crystals for ultrasonic transducers. IEEE Trans Ultrason Ferroelectr Freq Control. 1997; 44(5):1140–1147.
25. Ye ZG, Dong M. Morphotropic domain structures and phase transitions in relaxor-based piezo/ferroelectric $(1-x)Pb(Mg_{1/3}Nb_{2/3})O_3–xPbTiO_3$ single crystals. J Appl Phys. 2011; 87(5):2312–2319.
26. Zhang SJ, Luo J, Hackenberger W, Shrout TR. Characterization of $Pb(In_{1/2}Nb_{1/2})O_3–Pb(Mg_{1/3}Nb_{2/3})O_3–PbTiO_3$ ferroelectric crystal with enhanced phase transition temperatures. J Appl Phys. 2008; 104(6) art. no. 64106.
27. Tian J, Han PD, Huang XL, Pan HX, Carroll JF III, Payne DA. Improved stability for piezoelectric crystals grown in the lead indium niobate-lead magnesium niobate-lead titanate system. Appl Phys Lett. 2007; 91(22) art. no. 222903.
28. Sun P, Zhou QF, Zhu B, Wu D, Hu C, Cannata JM, Tian J, Han PD, Gao GF, Shung KK. Design and fabrication of PIN-PMN-PT single-crystal high-frequency ultrasound transducers. IEEE Trans Ultrason Ferroelectr Freq Control. 2009; 56(12):2760–2763. [PubMed: 20040413]
29. Chen R, Wu JC, Lam KH, Yao LH, Zhou QF, Tian J, Han PD, Shung KK. Thermal-independent properties of PIN-PMN-PT single-crystal linear-array ultrasonic transducers. IEEE Trans Ultrason Ferroelectr Freq Control. 2012; 59(12):2777–2784. [PubMed: 23221227]
30. IEEE Standard on Piezoelectricity. ANSI/IEEE Std; 1987. p. 176
31. Zhou QF, Xu XC, Gottlieb EJ, Sun L, Cannata JM, Ameri H, Humayun MS, Han PD, Shung KK. PMN-PT single crystal, high-frequency ultrasonic needle transducers for pulsed wave Doppler application. IEEE Trans Ultrason Ferroelectr Freq Control. 2007; 54(3):668–675. [PubMed: 17375836]
32. Cannata JM, Ritter TA, Chen WH, Silverman RH, Shung KK. Design of efficient, broadband single-element (20–80 MHz) ultrasonic transducers for medical imaging applications. IEEE Trans Ultrason Ferroelectr Freq Control. 2003; 50(11):1548–1557. [PubMed: 14682638]

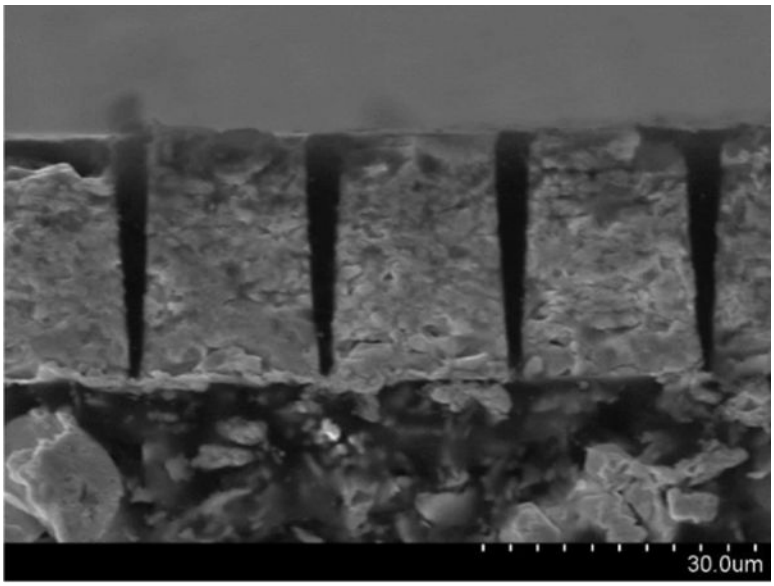

Fig. 1.
PIN-PMN-PT 1–3 composite with conductive backing.

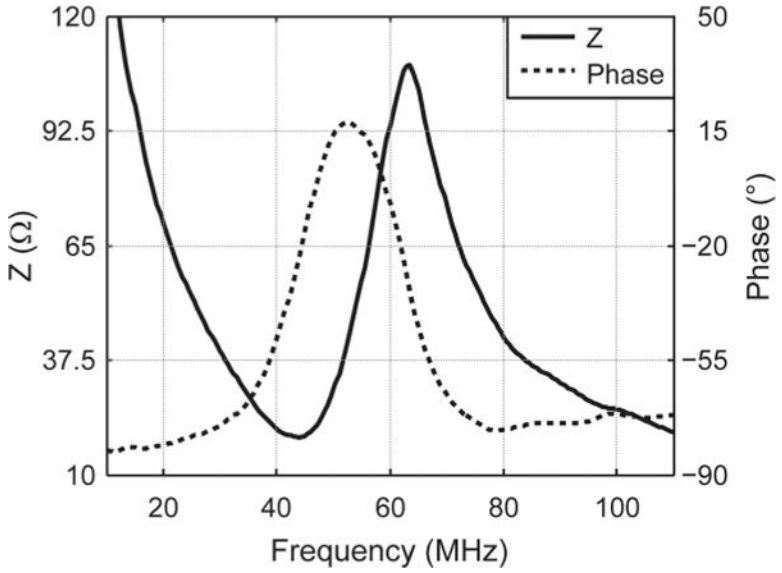

Fig. 2.
Electrical impedance and phase of a PIN-PMN-PT composite stack at room temperature.

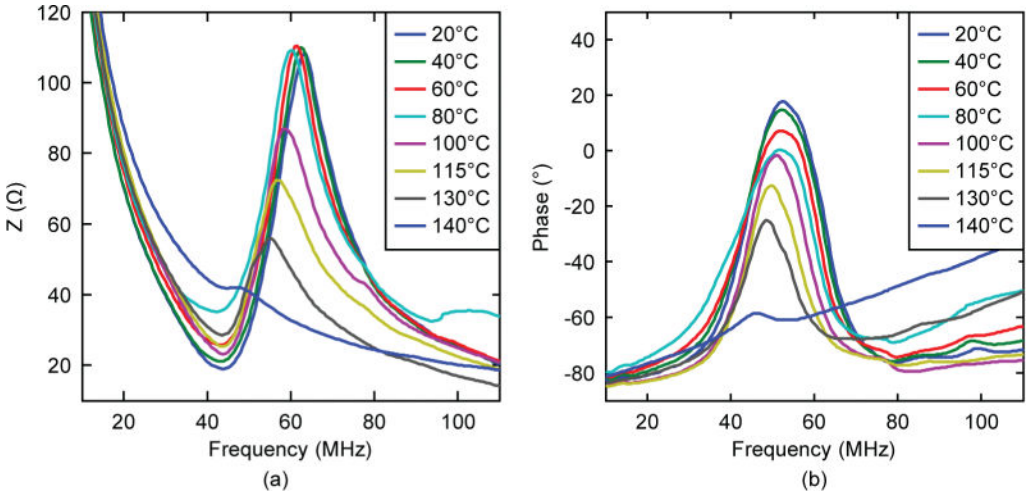

Fig. 3.

Temperature dependence of electrical impedance and phase of a PIN-PMN-PT composite stack.

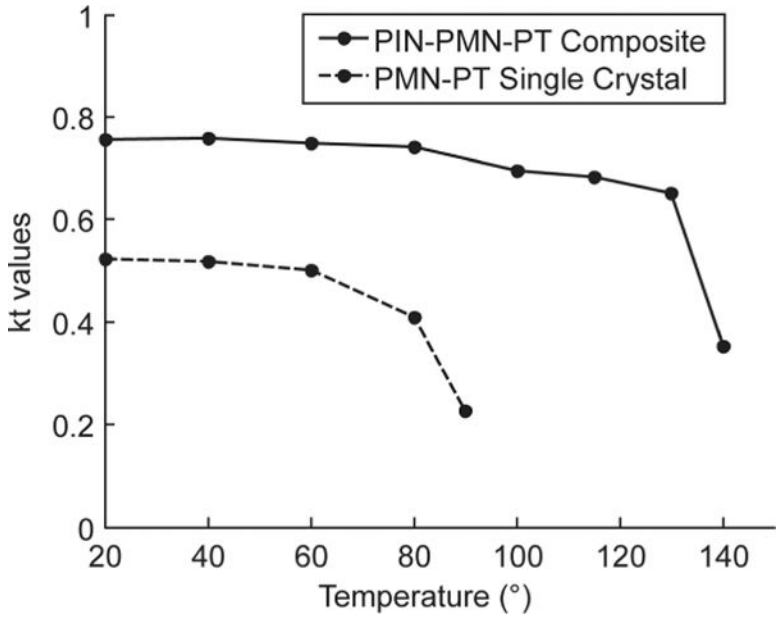

Fig. 4.

Temperature dependence of electromechanical coupling coefficient values of PIN-PMN-PT composite and PMN-PT single crystal.

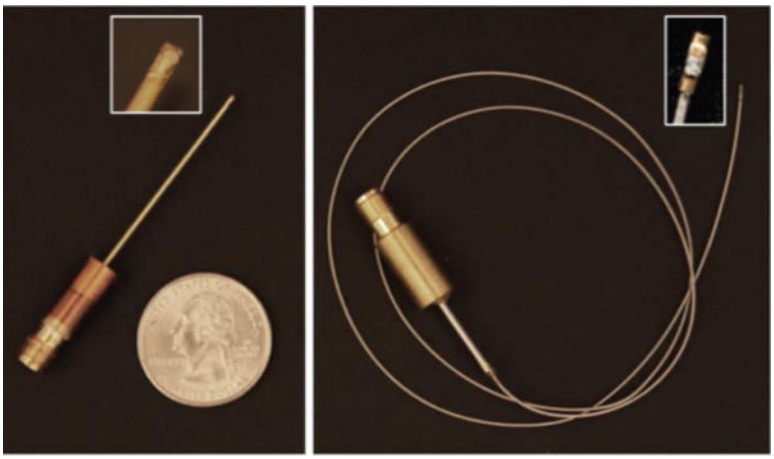

Fig. 5.
PIN-PMN-PT composite IVUS transducers: (a) needle type; and (b) flexible type.

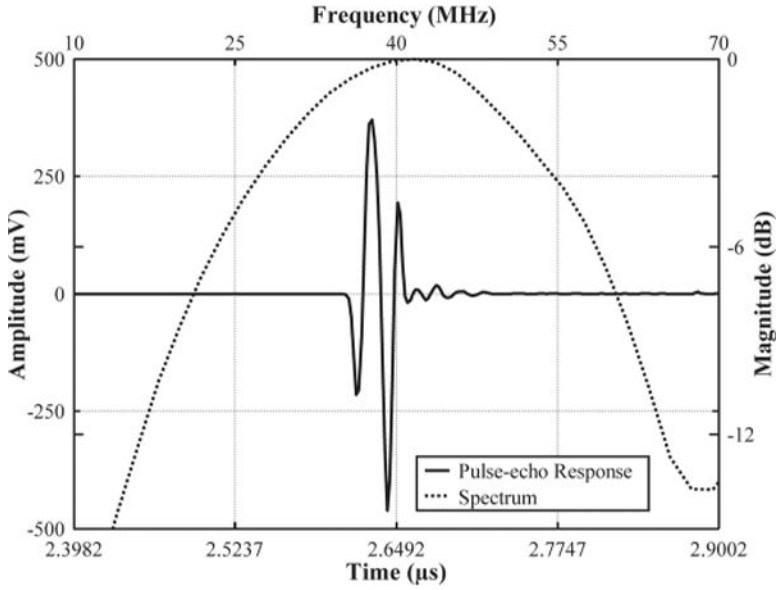

Fig. 6.

Pulse–echo measurement of a PIN-PMN-PT composite transducer.

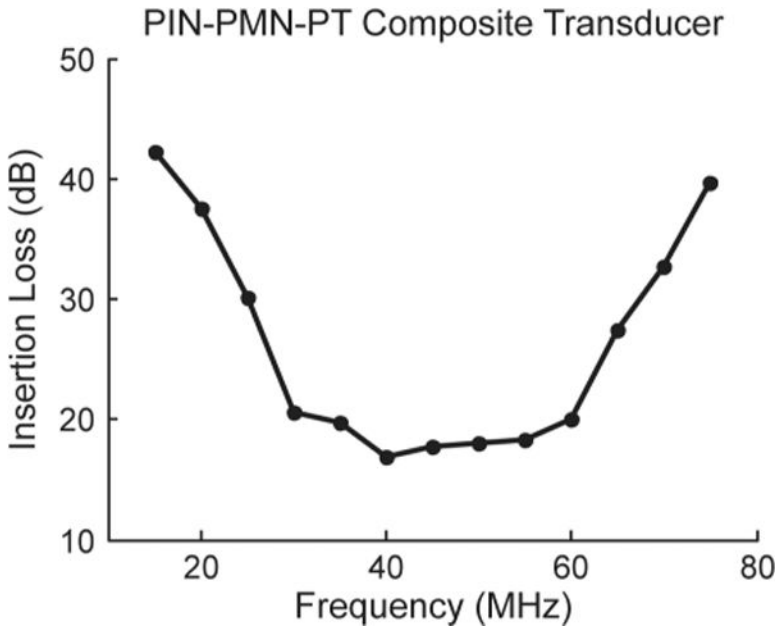

Fig. 7.
Two-way insertion loss measurement of a PIN-PMN-PT composite transducer.

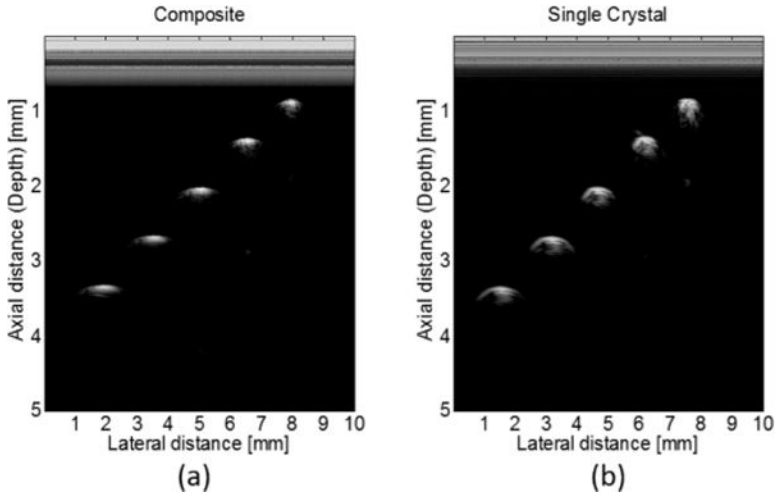

Fig. 8.

Wire phantom images from (a) PIN-PMN-PT composite transducer; and (b) PMN-PT single-crystal transducer.

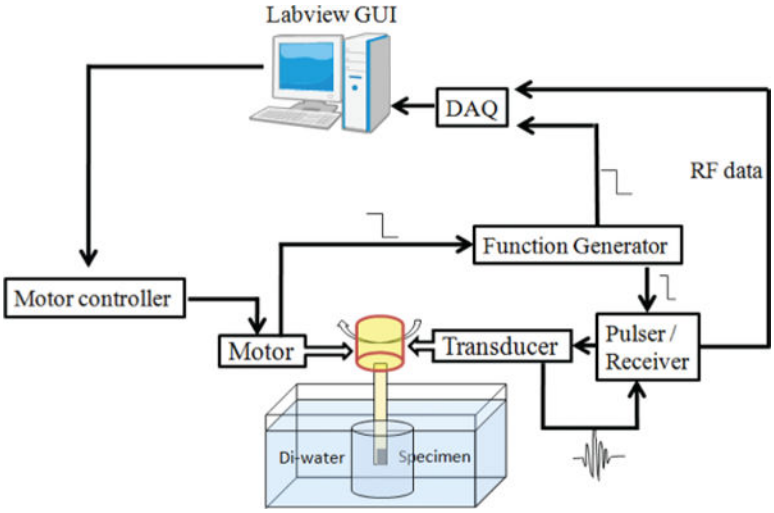

Fig. 9.
IVUS imaging system.

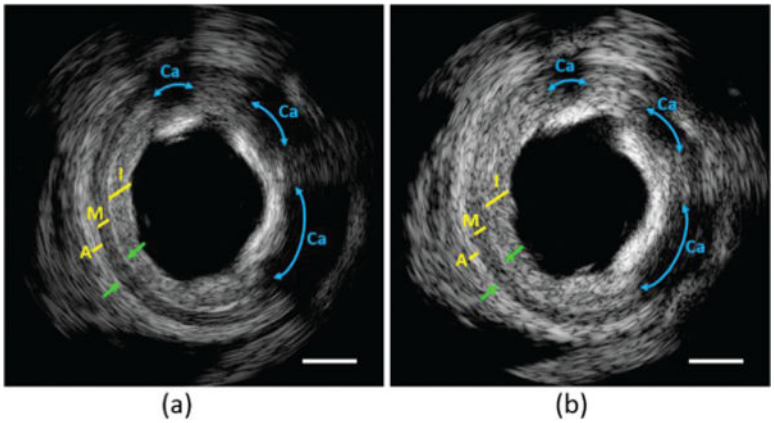

Fig. 10.

IVUS image of human coronary artery at 40 MHz from (a) PIN-PMN-PT composite transducer; and (b) PMN-PT single-crystal transducer. I = intima; M = media; A = adventitia; Ca = calcified plaque. Green arrows denote the boundaries of IM and MA. Scale bar is 1 mm.